Valence band alignment and hole transport in amorphous/crystalline silicon heterojunction solar cells

Mathias Mews,[1, a)] Martin Liebhaber,[1] Bernd Rech,[1] and Lars Korte[1]

Helmholtz-Zentrum Berlin, Institute of Silicon Photovoltaics, Kekuléstraße 5, D-12489 Berlin, Germany

(Dated: 26 June 2015)

To investigate the hole transport across amorphous/crystalline silicon heterojunctions, solar cells with varying band offsets were fabricated using amorphous silicon suboxide films. The suboxides enable good passivation if covered by a doped amorphous silicon layer. Increasing valence band offsets yield rising hole transport barriers and reduced device effciencies. Carrier transport by thermal emission is reduced and tunnel hopping through valence band tail states increases for larger barriers. Nevertheless, stacks of films with different band gaps, forming a band offset staircase at the heterojunction could allow the application of these layers in silicon heterojunction solar cells.

[a)] mathias.mews@helmholtz-berlin.de

Silicon wafer based solar cells provide most of today's global photovoltaic power generation. A number of technologies are competing for future market shares. Among those amorphous/crystalline silicon heterojunction (SHJ) solar cells[1] provide the highest potential efficiency,[2] mainly due to the very low defect density at the SHJ. However parasitic absorption in the amorphous silicon (a-Si:H) front contact and passivation layers is restraining their efficiency.[3] The total current density lost in 5 nm p-type a-Si:H is about 1.2 mA/cm^2 and about 0.6 mA/cm^2 are lost by absorption in 5 nm intrinsic a-Si:H.[3] Therefore the replacement of the front hole contact and the passivation layer with high band gap and low absorption a-Si:H alloys like amorphous, or microcrystalline silicon oxide (a-SiO$_x$:H)[4–7], or silicon carbide[8] is an ongoing research topic.

This letter focuses on the hole transport across the SHJ between a-Si:H, or a-SiO$_x$:H and crystalline silicon (c-Si). This interface serves as a model system for the application of high band gap layers, for reduction of parasitic absorption in SHJ solar cells.[1] A sketch of the band line-up at the SHJ between a p-type a-Si:H hole contact, an intrinsic a-SiO$_x$:H passivation layer and an n-type c-Si absorber is shown in Fig. 1. Holes generated in the (n)c-Si are directed towards the p/n-junction, where they have to overcome the valence band offset (ΔE_V) to enter the (i)a-SiO$_x$:H and the (p)a-Si:H layer. Values for ΔE_V at the SHJ were reported to be about 200 to 450 meV[9–11] and are no obstacle to carrier transport, although the exact carrier mechanism is still subject of discussion.[12–14]

Two possible transport paths exist. First, the holes can overcome the band offset barrier by thermionic emission. Secondly, they can tunnel into the a-Si:H passivation layer[12] and then travel by tunnel hopping[13] in its valence band tail states.[15] Tunnel hopping is expected to become increasingly important for increased ΔE_V[12] and decreasing electrical quality of the passivation layer.[15]

Fujiwara *et al.*[16] demonstrated the feasibility of a-SiO$_x$:H passivation and demonstrated that increasing CO_2 precursor gas fractions lead to decreasing fill factors (FF). Furthermore, studies on a-SiO$_x$:H passivation layers[7,17,18] and their application in solar cells[5] were conducted. Recently Seif *et al.*[4] reproduced the results of Fujiwara *et al.*[16] and employed device simulation to reason that an increasing oxygen content leading to a rise of ΔE_V may explain the decreasing FF due to a transport barrier, which impedes thermionic emission of holes across ΔE_V. Unfortunately Seif *et al.*[4] used stacks of a-SiO$_x$:H and a-Si:H and only changed the oxygen content of the top layer. Therefore ΔE_V at the SHJ may not have been changed

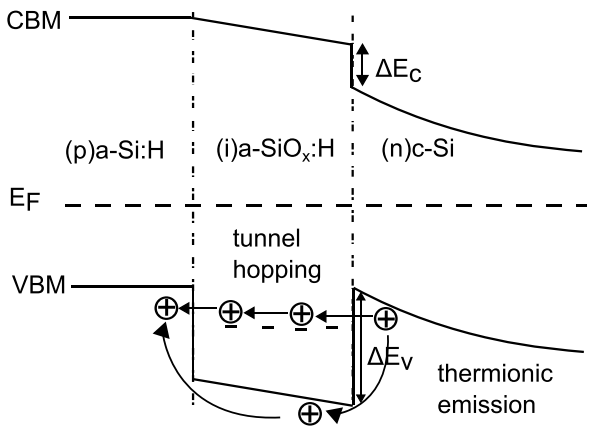

FIG. 1. Band line-up at the hole contact of amorphous/crystalline silicon heterojunction (SHJ) solar cells with an n-type c-Si absorber. Holes generated in the c-Si can traverse the SHJ by thermionic emission over the valence band offset (ΔE_V), or by tunnel hopping through the valence band tail states of the intrinsic amorphous silicon(oxide). They then travel in the (p)a-Si:H valence band and are collected at the external contacts. The sketch also shows the Fermi-level (E_F), valence band maximum (VBM), conduction band minimum (CBM) and conduction band offset (ΔE_C).

at all. Recently we determined ΔE_V at this interface for the full stoichiometry range.[19] This letter aims at combining band line-up measurements with device and passivation results to gain insight about the carrier transport across this junction.

To this end, (p)a-Si:H/(i)a-SiO$_x$:H/(n)c-Si/(i,n)a-Si:H solar cells were processed and characterized, as follows:

The substrates for solar cell preparation are 280 μm thick, polished phosphorous doped float-zone grown c-Si wafers with (111) surface orientation and a resistivity of 3 Ωcm. Wafers were cleaned using the RCA process and dipped in diluted hydrofloric acid (1 %, 2 min) before layer deposition. A-Si:H and a-SiO$_x$:H layers were deposited using plasma-enhanced chemical vapor deposition. Intrinsic a-SiO$_x$:H was prepared using 60 MHz excitation, a process pressure of 0.5 mbar, a substrate temperature of 175°C, an electrode distance of 2 cm, a plasma power density of 56 mW/cm^2, and a total gas flow of 15 sccm. The gas flow consisted of 5 sccm hydrogen, and a total of 10 sccm silane and CO_2. The a-Si:H layers were deposited using 10 sccm of silane and no CO_2. For the a-SiO$_x$:H layers, the CO_2 flow was raised in 1 sccm steps up to a value of 5 sccm, and the silane flow was decreased accordingly. For solar cell fabrication wafers were coated with 4 nm intrinsic a-Si:H and 8 nm n-type

a-Si:H on the backside and 5 nm intrinsic a-SiO_x:H and 8 nm p-type a-Si:H on the front side. The solar cells were then completed by ITO sputtering and metalization with Ti/Ag stacks. The full solar cell process is discussed elsewhere.[20]

Photoconductance decay and illumination dependent open circuit voltage (so-called SunsV_{OC}) measurements[21] were carried out in between various process steps.

ΔE_V of the a-SiO_x:H/c-Si-SHJs were determined using photoelectron spectroscopy in the constant-final-state-yield mode[22] and a procedure described elswhere.[10,11] The measurement of oxygen content and ΔE_V in these layers was discussed in an earlier publication.[19]

Numerical device simulation with AFORS-HET[23] was used to discuss the experimental data. The a-SiO_x:H layers were simulated using a model for a-Si:H with an electron affinity of 3.724 eV and a defect density consisting of two Gaussian defect densities of about $10^{14}\,cm^{-3}$ and band tails at the valence and conduction band. The band gap of the pure a-Si:H was assumed to be 1.68 eV. For a-SiO_x:H, it was increased to mirror the measured increase in valence band offset, holding the conduction band position constant. The Urbach energy (E_U) of the valence band tail was adjusted according to measured values[19] and the E_U of the conduction band tail was set to two thirds of the valence band E_U.[24]

Fig. 2a shows the evolution of ΔE_v for the layers used in this study. An increase in the oxygen fraction leads to an increase of ΔE_v. Additionally, Fig. 2b displays the evolution of the effective minority carrier lifetime in solar cell precursors with an intrinsic a-Si:H passivation and n-type a-Si:H contact layer on the back side, and an (i)a-SiO_x:H layer on the front side. The minority carrier lifetime decreases for increasing oxygen content, but rises drastically in the samples with higher oxygen concentrations after the deposition of an additional p-type a-Si:H layer on top of the (i)a-SiO_x:H layers. To further investigate this process the interface defect density was extracted from the injection dependence of the minority carrier lifetime.[25] The results are depicted in Fig. 2c. It is obvious that the lifetime gain is based on a decreased interface defect density (D_{it}) upon (p)a-Si:H deposition. Note, that the model applied for the extraction of the D_{it} assumes symmetrical samples and the samples in the present study were not symmetric. This may lead to an overestimation of the calculated D_{it}, if the D_{it} at the investigated interface is of the same order of magnitude as at the sample's backside. However the error is below 10 % for effective minority carrier lifetimes below 4 ms, since the backside passivation enables effective lifetimes of about 12 ms. The D_{it} at the SHJ interface is directly related to the Si bonding environment[26] and the

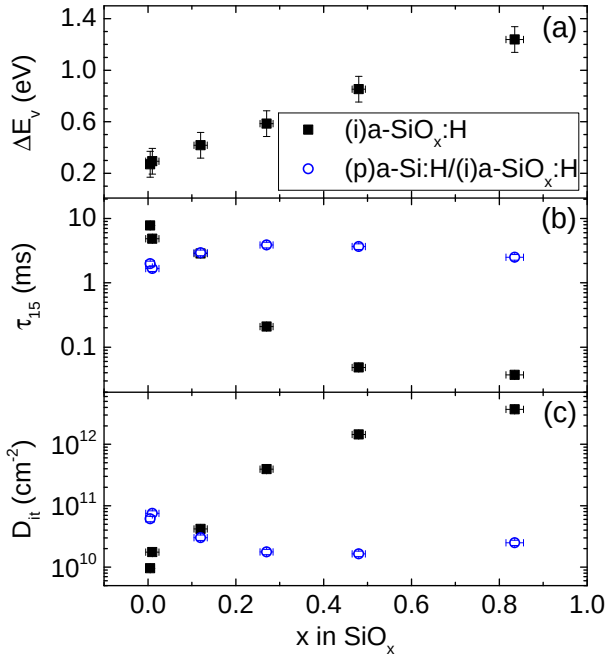

FIG. 2. Band alignment and interface passivation properties of amorphous silicon suboxide/crystalline silicon heterojunctions (a-SiO$_x$:H/c-Si-HJ) with different oxygen fractions. (a) Valence band offsets (ΔE_v) at the SHJ, as measured in our earlier study.[19] (b) Minority carrier lifetime at an injection level of 10^{15}cm^{-2} (τ_{15}) for c-Si passivated with a-SiO$_x$:H (black squares) and after subsequent deposition of a p-type a-Si:H layer on top of the a-SiO$_x$:H, measured on the same samples (empty blue circles). (c) a-SiO$_x$:H/c-Si-HJ interface defect density (D_{it}) of the same samples as in (b).

hydrogen density[9] at the interface. Since the temperature of the (p)a-Si:H deposition is too low to affect the Si bonding structure,[27] the decrease in D_{it} is likely due to an increase of the hydrogen density at the SHJ. It is conceivable that the additional hydrogen is provided by the plasma process during the (p)a-Si:H deposition.

The current-voltage (j(U)) curves of solar cells fabricated with these layer stacks are depicted in Fig. 3a. An increase of ΔE_V at the hole contact leads to the development of s-shaped j(U) curves. This behavior was predicted on the basis of numerical simulations,[4,12,13] but no systematic experimental evidence has been presented so far.

Fig. 3b depicts the solar cell's open circuit voltages (V_{OC}), together with the implied open circuit voltages (iV_{OC}),[21] as extracted from photoconductance decay measurements prior to ITO depositions.

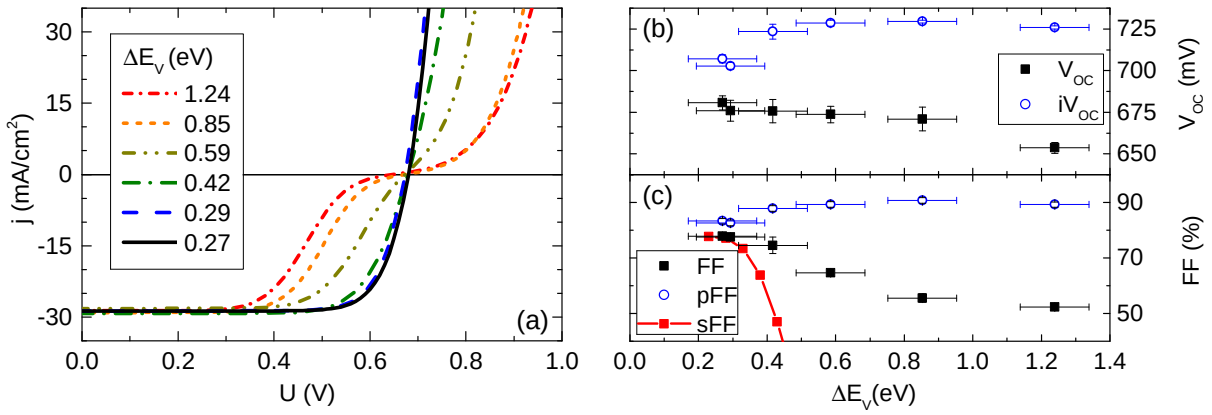

FIG. 3. Influence of ΔE_V at the SHJ on (a) the current-voltage (j(U)) characteristics of SHJ solar cells with different a-SiO_x:H passivation layers, (b) the open circuit voltage (V_{OC}) and implied V_{OC} (iV_{OC}) and (c) the solar cell fill factor (FF), SunsV_{OC} pseudo fill factor (pFF), simulated fill factor (sFF) of the same solar cells.

The V_{OC} of the solar cells decreases slowly for increasing ΔE_V. Increasing the oxygen fraction in a-SiO_x:H layers increases the layer porosity and the density of Dihydrides and hydrogen filled voids.[18] Furthermore hydrogen in Dihydride configuration and in voids is more mobile, than Monohydrides, and is driven out of the layer during ITO sputtering.[28] This could explain why layers with higher oxygen contents degrade stronger during follow up processes than layers with lower oxygen contents and show decreased minority carrier lifetimes after ITO sputtering.

Fig. 3c displays the dependence of fill factors (FF) and pseudo fill factors (pFF) of the solar cells on ΔE_V. The pFF was measured using SunsV_{OC}, a method that induces no external current flow in the device and therefore reflects the maximum FF excluding carrier transport related effects. The FF decreases with increasing ΔE_V, whereas the pFF is slightly increased. Consequently the decreasing FF can be related to a transport barrier and effects of e.g. decreased passivation at low injection can be excluded.[29–32] The reason for the increase of the pFF with decreasing FF is unknown, although similar results have been reported before.[33,34] One possibility is, that the transport barrier increases the passivation at low injection densities and no net current flow.

Numerical simulations were used to simulate FF (sFF) values for the same devices, which are also plotted in Fig. 3b. Obviously the simulation overestimates the influence of ΔE_V on the FF. Since the FF of the solar cells decreases with increasing ΔE_V, while the pFF increases,

it can be concluded that the increasing ΔE_V creates a transport barrier. Furthermore, the overestimation of the FF degradation with increasing ΔE_V in the numerical simulation gives further insight into the carrier transport mechanisms. Only thermionic emission is employed to simulate the transport across the SHJ. The assumption of thermionic emission as the main transport mechanism in SHJ solar cells is commonly used in simulation studies.[4,35–37] However, the results depicted in Fig. 3 imply that another transport path becomes prevalent once ΔE_V is increasing well above the thermal energy of carriers at 300 K. Indeed, there are a few simulation studies which ascribe a significant importance to tunneling through the interface[12,14] or tunnel hopping in valence band tail states[13,38] in the a-Si:H layers.

Comparing the results of these studies and our simulations to the experimental data in Fig. 3, it is clear that all simulations of the hole transport using only thermionic emission overestimate the detrimental influence of high ΔE_V.[14,35,36] In contrast, simulations that include tunnel hopping in a-Si:H, or its alloys show good agreement with our experimental data.[12,13] Kanevce and Metzger[12] discuss the transport across the interface between n-type a-Si:H and p-type c-Si in detail. Their findings include that a significant fraction of the current flow across the SHJ is delivered via tunneling into and tunnel hopping in the a-Si:H layers. Their simulated j(U) curves for varying band offsets at the minority carrier contact qualitatively match the experimental findings of the present study. Note, that their simulations treat devices of inverse polarity compared to our study. Still it is reasonable to compare these results to the present study, as the respective electron and hole mobilities are of the same order of magnitude and the band offset ranges are comparable.

All in all, for minority carrier band offsets above 400 meV, it is mandatory to consider tunneling into and tunnel hopping in the a-Si:H layer to obtain sufficient agreement of experimental data and simulation.

The presented experimental results have important implications for the application of high band gap alloys at the hole contact of SHJ solar cells,[5–8] since all Si alloys reported in literature feature high ΔE_V values.[11,19,39,40] This is most unfortunate, since the application of those high band gap alloys is desirable to reduce the parasitic absorption in front side minority carrier contacts.[3] However one way to enable the application of high band gap alloys may be the application of a stack of materials. This stack could comprise an a-Si:H layer with a moderate ΔE_V of about 200 to 300 meV and a second layer with a higher band gap. This splits the effective ΔE_V between two interfaces and thermionic emission across

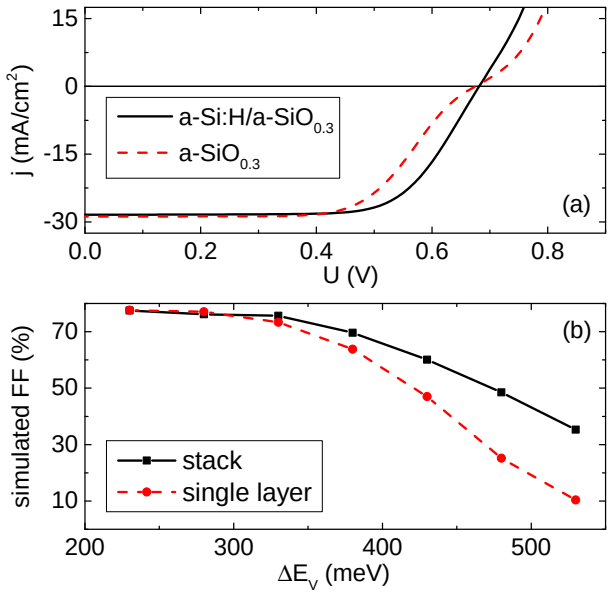

FIG. 4. (a) j(U)-curves of solar cells with a 5 nm thick a-$SiO_{0.3}$:H passivation layer and a solar cell with a passivation layer stack consisting of 2 nm a-Si:H and 3 nm a-$SiO_{0.3}$:H. The ΔE_V of the a-Si:H/c-Si interface is about 270±50 meV, whereas ΔE_V between the a-$SiO_{0.3}$:H and the c-Si is about 585±50 meV. (b) FF extracted from simulated j(U) curves using thermionic emission over an a-SiO_x:H/c-Si interface with variable ΔE_V and the same simulation for a stack of a-SiO_x:H/a-Si:H/c-Si. For the stack, the total ΔE_V is plotted on the abscissa. ΔE_V for the a-Si:H/c-Si-SHJ in the stack is 270 meV.

each single interface is facilitated. Thus, hole transport is enabled across a valence band staircase, which allows carrier transport across a larger ΔE_V, which charge carriers could not overcome efficiently in a single step. Additionally, stacks comprising even more layers or graded layers are a possibility.

Solar cells comprising hole contact passivation layer stacks of 2 nm a-Si:H and 3 nm a-$SiO_{0.3}$:H were fabricated to test this approach. The band offset between a-Si:H and c-Si is 270±50 meV, while ΔE_V at the a-$SiO_{0.3}$:H/c-Si SHJ is about 585±50 meV.[19] The j(U)-characteristics of such a solar cell is shown in Fig. 4a together with a reference. The solar cell in which the holes have to traverse ΔE_V in a single step displays a clear transport barrier, as reflected in the s-shaped j(U)-curve and a fill factor of only 63 %. In contrast, there is no transport barrier, albeit a somewhat reduced FF of 70 %, for the solar cell in which ΔE_V is divided between two interfaces. The solar cells with an a-Si:H passivation layer have a FF

of 78 %. Note that the V_{OC}'s of the two cells are identical, indicating comparable interface defect densities. Numerical simulations were conducted to further illustrate this concept. Solar cells comprising different ΔE_V at the SHJ and devices with the same total ΔE_V, but a 2 nm interlayer with a ΔE_V of 270 meV were simulated using only thermionic emission as transport mechanism. The FF values from these simulations are shown in Fig. 4b. As expected, the application of a material stack does not change the trend of decreasing FF with increasing ΔE_V, but increases the FF for a given valence band offset. While the experimental stack will likely feature increased hopping currents, due to the only 3 nm thin oxide layer, it still illustrates the concepts. Furthermore, since the simulations do not include hopping the reason for the improved FFs is most likely more efficient thermionic emission along the layer stack, as compared to the single interface with one big valence band offset. In conclusion it was possible to demonstrate the importance of an appropriate band alignment at the p-n-junction of SHJ solar cells. Specifically, an increased ΔE_V at the hole contact of SHJ solar cells gives rise to a transport barrier. Moreover, the increasing transport barrier leads to an increasing contribution of tunnel hopping through valence band tail states and tunneling transport and a decreasing contribution of thermionic emission, which in turn decreases device efficiencies. The latter effect is a general problem for high band gap a-Si:H alloys as hole contacts of SHJ solar cells. An approach to mitigate this problem by applying a stack of at least two layers with a step-like increase of ΔE_V at the SHJ was presented. The improved FFs of the solar cells with stacked passivation layers highlight a viable approach towards the application of high band gap a-Si:H alloys as hole contact layers in SHJ solar cells. This concept is promising for the combination of a passivation layer with a moderate band gap and a high band gap hole contact.

ACKNOWLEDGMENTS

The authors would like to thank Thomas Lußky, Erhard Conrad, Kerstin Jacob and Mona Wittig for technical assistance. Financial support was provided by the European Commission through the FP7-ENERGY Project HERCULES (Grant No. 608498) and the German Federal Ministry for Research and Education through the project SISSY (Grant No. BMBF-03SF0403).

REFERENCES

[1]S. De Wolf, A. Descoeudres, Z. C. Holman, and C. Ballif, Green **2**, 7 (2012).

[2]M. Taguchi, A. Yano, S. Tohoda, K. Matsuyama, Y. Nakamura, T. Nishiwaki, K. Fujita, and E. Maruyama, IEEE J. Photovolt. **4**, 96 (2014).

[3]Z. C. Holman, A. Descoeudres, L. Barraud, F. Z. Fernandez, J. P. Seif, S. De Wolf, and C. Ballif, IEEE J. Photovolt. **2**, 7 (2012).

[4]J. P. Seif, A. Descoeudres, M. Filipic, F. Smole, M. Topic, Z. C. Holman, S. De Wolf, and C. Ballif, J. Appl. Phys. **115**, 024502 (2014).

[5]K. Ding, U. Aeberhard, F. Finger, and U. Rau, J. Appl. Phys. **113**, 134501 (2013).

[6]L. Mazzarella, S. Kirner, B. Stannowski, L. Korte, B. Rech, and R. Schlatmann, Appl. Phys. Lett. **106**, 023902 (2015).

[7]T. Mueller, S. Schwertheim, M. Scherff, and W. R. Fahrner, Appl. Phys. Lett. **92**, 033504 (2008).

[8]D. Zhang, D. Deligiannis, G. Papakonstantinou, R. van Swaaij, and M. Zeman, IEEE J. Photovolt. **4**, 1326 (2014).

[9]M. Mews, T. F. Schulze, N. Mingirulli, and L. Korte, Appl. Phys. Lett. **102**, 122106 (2013).

[10]L. Korte and M. Schmidt, J. Appl. Phys. **109**, 063714 (2011).

[11]T. F. Schulze, F. Ruske, B. Rech, and L. Korte, Phys. Rev. B **83**, 165314 (2011).

[12]A. Kanevce and W. K. Metzger, J. Appl. Phys. **105**, 094507 (2009).

[13]M. W. M. van Cleef, R. E. I. Schropp, and F. A. Rubinelli, Appl. Phys. Lett. **73**, 2609 (1998).

[14]M. Rahmouni, A. Datta, P. Chatterjee, J. Damon-Lacoste, C. Ballif, and P. Roca i Cabarrocas, J. Appl. Phys. **107**, 054521 (2010).

[15]P. G. Le Comber and W. E. Spear, Phys. Rev. Lett. **25**, 509 (1970).

[16]H. Fujiwara, T. Kaneko, and M. Kondo, Appl. Phys. Lett. **91**, 133508 (2007).

[17]T. Mueller, S. Schwertheim, and W. R. Fahrner, J. Appl. Phys. **107**, 014504 (2010).

[18]F. Einsele, W. Beyer, and U. Rau, J. Appl. Phys. **112**, 054905 (2012).

[19]M. Liebhaber, M. Mews, T. F. Schulze, L. Korte, B. Rech, and K. Lips, Appl. Phys. Lett. **106**, 031601 (2015).

[20]M. Mews, C. Leendertz, M. Algasinger, S. Koynov, and L. Korte, Phys. Status Solidi RRL. **8**, 831 (2014).

[21]R. A. Sinton and A. Cuevas, Appl. Phys. Lett. **69**, 2510 (1996).

[22]M. Sebastiani, L. Di Gaspare, G. Capellini, C. Bittencourt, and F. Evangelisti, Phys. Rev. Lett. **75**, 3352 (1995).

[23]R. Varache, C. Leendertz, M. Gueunier-Farret, J. Haschke, D. Munoz, and L. Korte, Sol. En. Mat. Sol. Cells **141**, 14 (2015).

[24]K. Winer, I. Hirabayashi, and L. Ley, Phys. Rev. B **38**, 7680 (1988).

[25]C. Leendertz, N. Mingirulli, T. F. Schulze, J.-P. Kleider, B. Rech, and L. Korte, Appl. Phys. Lett. **98**, 202108 (2011).

[26]H. Fujiwara and M. Kondo, Appl. Phys. Lett. **90**, 013503 (2007).

[27]S. De Wolf and M. Kondo, Appl. Phys. Lett. **91**, 112109 (2007).

[28]B. Demaurex, S. D. Wolf, A. Descoeudres, Z. C. Holman, and C. Ballif, Appl. Phys. Lett. **101**, 171604 (2012).

[29]R. Rößler, C. Leendertz, L. Korte, N. Mingirulli, and B. Rech, J. Appl. Phys. **113**, 144513 (2013).

[30]K.-U. Ritzau, M. Bivour, S. Schrer, H. Steinkemper, P. Reinecke, F. Wagner, and M. Hermle, Sol. En. Mat. Sol. Cells **131**, 9 (2014).

[31]B. Macco, D. Deligiannis, S. Smit, R. A. C. M. M. van Swaaij, M. Zeman, and W. M. M. Kessels, Semicond. Sci. Technol. **29**, 122001 (2014).

[32]B. Demaurex, J. P. Seif, S. Smit, B. Macco, W. Kessels, J. Geissbuhler, S. De Wolf, and C. Ballif, IEEE J. Photovolt. **4**, 1387 (2014).

[33]M. Bivour, M. Reusch, S. Schröer, F. Feldmann, J. Temmler, H. Steinkemper, and M. Hermle, IEEE J. Photovolt. **4**, 566 (2014).

[34]C. Battaglia, S. M. de Nicolas, S. De Wolf, X. Yin, M. Zheng, C. Ballif, and A. Javey, Appl. Phys. Lett. **104**, 113902 (2014).

[35]M. Cleef, F. Rubinelli, R. Rizzoli, R. Pinghini, R. Schropp, and W. F. Weg, Jpn. J. Appl. Phys. **37**, 3926 (1998).

[36]V. Ai Dao, Y. Lee, S. Kim, J. Cho, S. Ahn, Y. Kim, N. Lakshminarayan, and J. Yi, J. Electrochem. Soc. **158**, H1129 (2011).

[37]A. Datta, M. Rahmouni, M. Nath, R. Boubekri, P. R. i Cabarrocas, and P. Chatterjee, Sol. En. Mat. Sol. Cells **94**, 1457 (2010).

[38]R. S. Crandall, E. Iwaniczko, J. V. Li, and M. R. Page, J. Appl. Phys. **112**, 093713 (2012).

[39]T. M. Brown, C. Bittencourt, M. Sebastiani, and F. Evangelisti, Phys. Rev. B **55**, 9904 (1997).

[40]J. M. Essick, Z. Nobel, Y.-M. Li, and M. S. Bennett, Phys. Rev. B **54**, 4885 (1996).